UDC 551.554:551.557(966.1)"1967.03-04"

THE PLANETARY BOUNDARY LAYER WIND OVER CHRISTMAS ISLAND

MARIANO A. ESTOQUE

Rosenstiel School of Marine and Atmospheric Sciences, University of Miami, Coral Gables, Fla.

ABSTRACT

Wind observations in the planetary boundary layer over an atoll near the Equator were made using the double-theodolite pilot balloon method. The observed mean wind profile is representative of boundary layer flow over a homogeneous surface with a very low value of the Coriolis parameter. The wind is predominantly easterly with a small backing with height. Analysis of the wind profile suggests that the component of motion along the east-west direction is approximately geostrophic; however, the component along the north-south direction is highly nongeostrophic. The analysis also indicates that the change in the wind direction with height is controlled mainly by the height variation of the horizontal pressure gradient.

1. INTRODUCTION

This report summarizes the results of pilot balloon observations made during the Line Island Experiment of March and April 1967. The observational site, Christmas Island, has two outstanding characteristics. It is located almost over the Equator (2°N, 157°W), and it is literally an isolated speck of land surrounded by a vast ocean. Thus, the planetary boundary layer wind over the site should be typical of conditions with small Coriolis parameter and horizontally uniform surface.

Our observational study is patterned after one that was conducted in the trades over Anegada Island (15°N, 64°W) by Charnock et al. (1956). Their observations consisted of 466 double-theodolite pilot balloon soundings on 15 separate days over a 27-day observational period. Balloons were released at intervals of 5 to 15 min, each balloon rising at the rate of about 150 m min^{-1}. Readings of the azimuth and vertical angles were made every 20 s. Using these readings, they calculated the three components of the wind for 50-m layers.

Some of the important results of the Anegada study are:

1. The wind veered with height through 24° in the first 1350 m.
2. The acceleration terms were negligible compared to the Coriolis, pressure gradient, and friction terms.
3. With respect to the perturbing effect of the island, they found that winds measured on the upwind shore were fairly representative of those over the open ocean.

It was our original intention to follow the same procedure of observations and analysis used in the Anegada study to test the validity of the above-mentioned results for Christmas Island. Unfortunately, the observations at Christmas Island were not sufficiently accurate for the calculation of the eddy components and the vertical velocities. Individual soundings did not give reliable estimates of the wind. However, the average of several soundings appear to yield reasonable wind profiles. Our report will, therefore, be concerned only with the average wind profiles.

2. DESCRIPTION OF THE OBSERVATIONAL SITE

Christmas Island is one of 11 atolls, collectively known as the Line Islands. They straddle the Equator between 6°N and 11°S about 1,000 mi south of the Hawaiian Islands (fig. 1). The island is shaped like a single-headed wrench (fig. 2) that is oriented along a southeast-northwest direction with its head at the northwest end. It is about 30 mi long. At the northwest end, it is 15 mi wide; at the southeast end, it is only 5 mi wide. There is a large lagoon at the northwest end and many smaller lagoons in the interior. The ground consists of coral sand and coral rock. Its average elevation is 15 ft. The highest elevations, located at the west end, are approximately 40 ft above sea level.

The double-theodolite observing site was located at Northeast Point (NE PT). As shown in figure 2, NE PT is very well exposed to the oceanic trades which are predominantly easterly. The ground at the site is about 7 ft above mean sea level. It is flat, open, and treeless. The only vegetation in this area is moderately sparse shrubbery from 3 to 5 ft high.

3. METEOROLOGICAL CONDITIONS

Christmas Island is located within the trades which are predominantly easterly during the entire year. Climatological data indicate that the average surface wind speed is about 10 kt. They also indicate that the trades are relatively deep, extending up to the 600-mb level. During the period of observations, March and April 1967, the intertropical convergence zone was located about 500 km north of Christmas Island. Hence, the atmosphere over the island was relatively undisturbed. Only two significant disturbances occurred, one on March 13 and the other on March 20. These two disturbances produced most of the rainfall during the period of observation. April was a drier month; it was also characterized by weaker winds.

The perturbing effect of the island on the prevailing flow pattern is important in relation to our attempt to

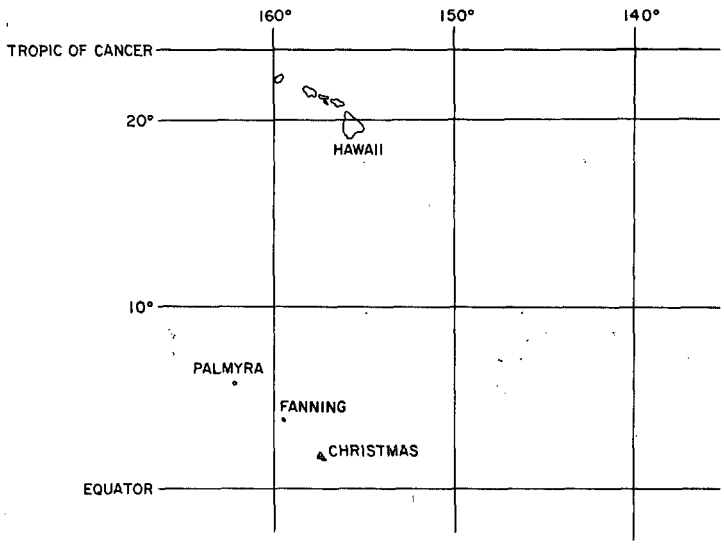

FIGURE 1.—Location map for Christmas Island.

obtain wind profiles representative of the oceanic trades. To assess the magnitude of this effect, we examined the diurnal variations in the meteorological observations at the island. Figure 3 shows the average diurnal variations of the surface temperature and the cloudiness observations at NE PT for the period of study. It may be seen that there is a distinct diurnal effect of the island heating. The amplitude of the surface temperature variation, approximately 3.5°F, is relatively small. The corresponding diurnal wind speed variations are shown in figure 4, separately for March and April. For comparison, the observations at London, a leeward station, are also shown in the same diagram. It is interesting to note that NE PT has a smaller amplitude in the surface wind speed variation than does London. This is simply due to the fact that the former is very well exposed to the oceanic trades. Note also that the diurnal variation at NE PT for March is practically negligible. This must be associated with the

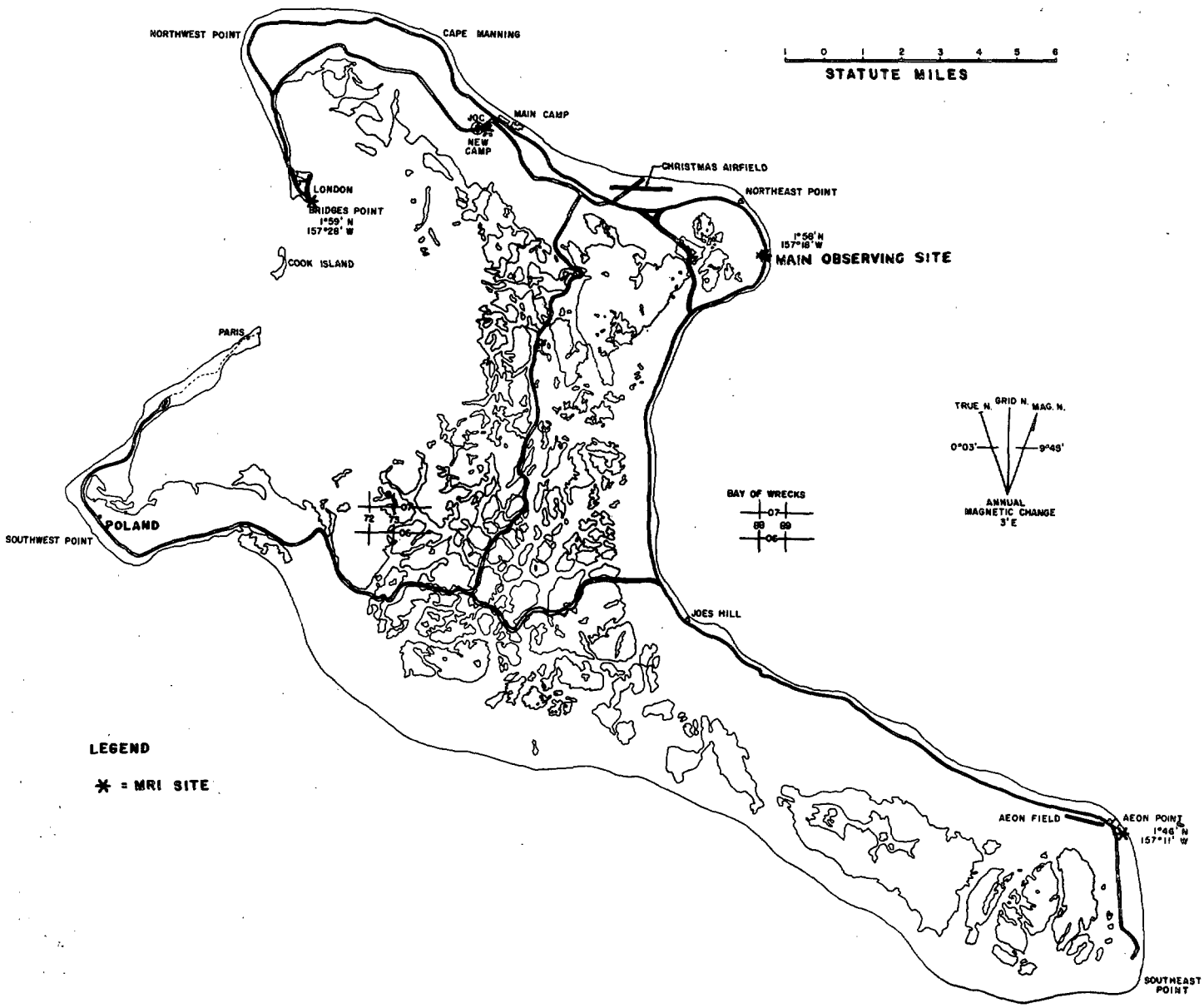

FIGURE 2.—Observing sites on Christmas Island.

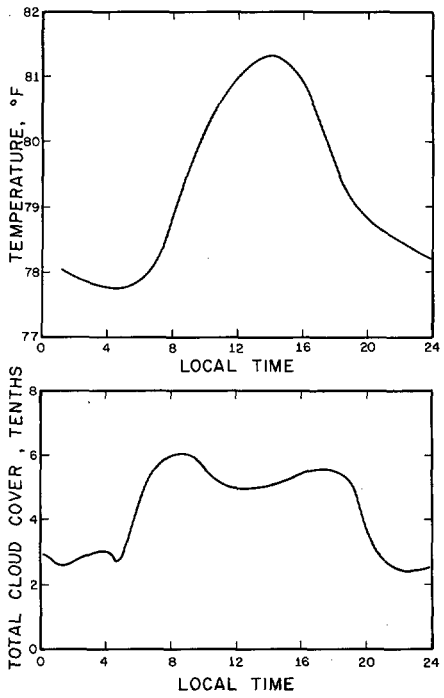

FIGURE 3.—Diurnal variations of surface temperature and cloud cover at Northeast Point on Christmas Island.

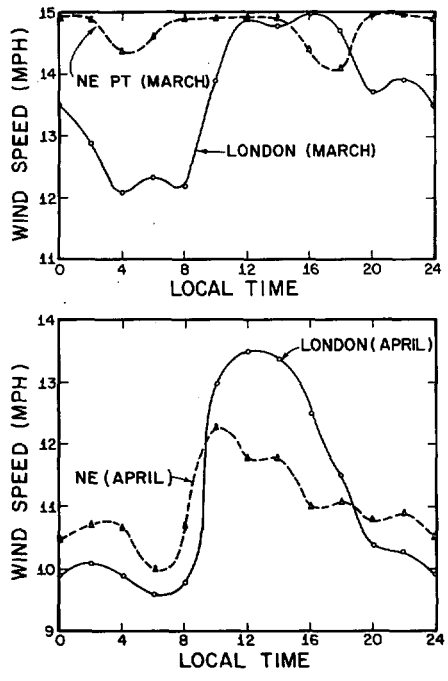

FIGURE 4.—Diurnal surface wind variations over Christmas Island.

stronger winds for this month. The amplitude of the diurnal surface wind speed variation for April is approximately 2 mi hr^{-1}. It is expected that the amplitude decreases with height. Hence, one may conclude that the pilot balloon observations should give winds that are fairly representative of those over the open ocean.

TABLE 1.—*Record of pilot balloon observations during March and April 1967*

Observing period	Date	Local time	No. of soundings
1	Mar. 5	0441-1115	19
2	7	0620-1200	18
3	8	0400-1200	24
4	9	0520-1200	18
5	10	0400-1200	24
6	14	0800-1600	24
7	16	0800-1600	22
8	21	1320-2040	20
9	22	1300-2100	22
10	23	1300-2100	22
11	27-28	2100-0440	21
12	28-29	2120-0500	22
13	29-30	2100-0420	20
14	Apr. 1	0800-1600	22
15	3	1300-1040	20
16	4	1300-2100	21
17	6-7	2100-0500	21
18	7-8	2100-0400	18
19	13	0400-1200	20
20	15	1320-2040	20
21	17	0800-1600	20
22	18	0820-1600	19
23	19	0800-1600	23
24	20-21	2100-0220	17

TABLE 2.—*Distribution of maximum height observed*

Height (m)	0-500	500-1000	1000-1500	1500-2000	2000-2500	Over 2500
Percentage	3	17	17	19	40	4

4. THE MEASUREMENTS

Pilot ballon observations were made between Mar. 5 and Apr. 21, 1967. There were 24 observing periods. Table 1 shows the dates of the observing periods and the local times of the ascents. The number of soundings per observational period ranged between a minimum of 18 to a maximum of 24; the average number is 21. There were about twice as many day as night releases. The distribution of heights up to which the ballons were followed is shown in table 2.

The baseline is 1 km long and oriented along a north-south direction, roughly parallel to the shoreline. The distance between the baseline and the water's edge is approximately 50 m. The balloons were released at a point in which azimuths are 188.1° and 352.0° from the north and the south stations, respectively. This point is 100 m west of the baseline. The balloons were released at intervals of 20 min during every observational period, which averaged 7 hr each. The elevation and azimuth angles were read to an accuracy of 0.1° at intervals of 20 s. The average ascent rate of the balloons was about 300 m min^{-1}.

From each pair of azimuth angles, the horizontal coordinates of the balloon were computed; each of the two elevation angles yields a separate estimate of the height, z_s and z_N. The final value of the estimates was assumed to be the average of z_s and z_N. The difference between the two values is a measure of the inaccuracy of the observations.

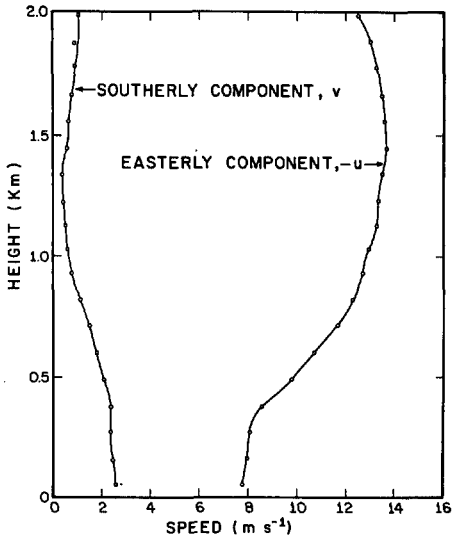

FIGURE 5.—Wind components averaged over all observations.

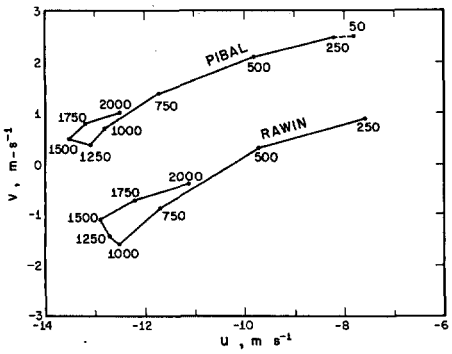

FIGURE 6.—Wind hodograph averaged over all observations. The numbers indicate elevations in meters above the surface.

A preliminary computation of the coordinates of the balloon with the raw data (with missing angles interpolated) gave large values of the difference, $|z_S - z_N|$. The values were used to detect obvious errors associated with the reading and the recording of the angles. By correcting the errors subjectively, we obtained a set of corrected angles. These angles were used in the final computation of the balloon coordinates and the corresponding velocities. It should be mentioned, however, that in spite of the corrections, the errors $|z_S - z_N|$ were still large. In many soundings, differences of as much as a few hundred meters still remained, especially at upper elevations. The average value was of the order of tens of meters which corresponds to an error in the velocity of the order of meters per second.

5. THE MEAN WIND PROFILE

The distribution of the mean wind (averaged over all observations) with height is shown in figure 5. It is seen that the easterly component increases with height to a maximum of 13.5 m s^{-1} at 1.5 km. Above this level, the speed decreases and finally becomes westerlies at about 5 km as indicated by rawin observations. The north-south component is southerly and is on the average an order of magnitude smaller. It decreases with height and reaches a minimum of 0.5 m s^{-1} at about the same level of the maximum in the easterly component. It appears that the wind does not approach a constant value in accordance with the customary boundary layer concept. This appears to be due primarily to the change in the horizontal pressure gradient with height.

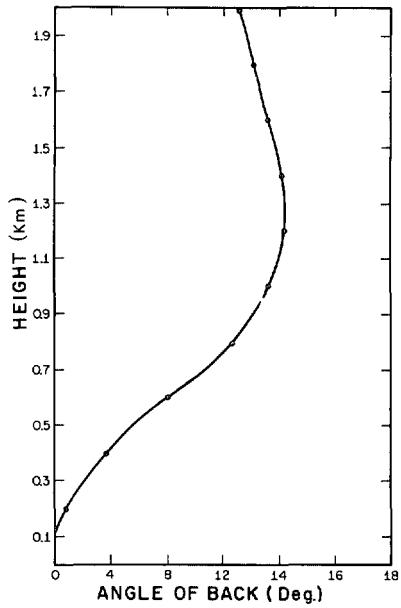

FIGURE 7.—Backing of the average wind relative to the wind at the 100-m level.

The wind is plotted as a hodograph in figure 6. Also shown on the diagram is the corresponding wind as observed with rawin. The rawin hodograph represents an average of 245 soundings. By comparing the two hodographs, one notes a systematic difference of approximately 10° in the wind directions. This is probably due to an error in the orientation of the azimuth measurements. Unfortunately, it is not possible to determine which measurement is in error.

The hodographs show the wind backing instead of veering with height. This is contrary to the normal turning of wind in the Northern Hemisphere. The angle of turn with respect to the wind vector at the 100-m level is shown in figure 7. The diagram shows a maximum angle of backing (15°) at about 1.3 km. It is clear that the mean wind profile over Christmas Island departs radically from the customary Ekman spiral. This fact is not entirely unexpected. The tentative explanation for this departure is the variation of the horizontal pressure gradient with height. This matter will be analyzed further in a later section.

We have already noted earlier the existence of a small diurnal wind variation induced by the island heating at

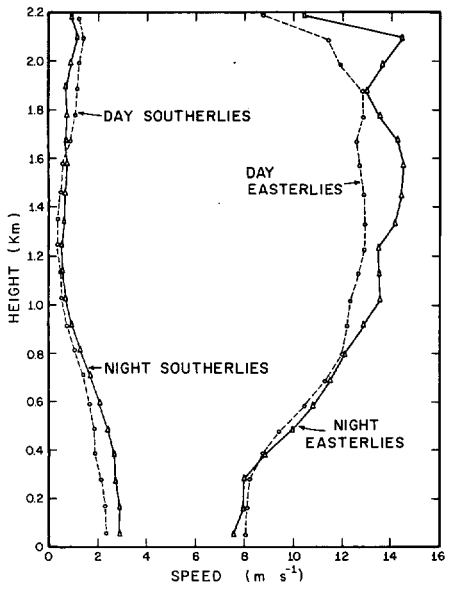

FIGURE 8.—Daytime and nighttime averages of the wind.

surface anemometer level. An attempt was made to determine the magnitude of this variation at upper levels by categorizing the observations into day and night soundings. The average wind profiles corresponding to these two categories are shown in figure 8. The difference between the two profiles is small, the large differences occurring at upper levels. On the basis of the available data, it is not possible to determine definitely whether these differences are due to diurnal effects. But the data appear to indicate that the night soundings were made during periods with relatively stronger easterlies. Thus, the differences between the two profiles are most probably due to inadequate sampling and not associated with real diurnal effects.

The wind profiles averaged for each of the 24 observational periods (fig. 9) are similar to the average profiles for all periods of observations described in the preceding section. The easterlies generally increase with height up to the 1.5-km level. The southerly component is always small. Profiles that deviate much from this average profile are few. An example of such a profile is the one within figure 9 for Apr. 18, 1967, at 0820–1600 LCT. This day was characterized by more cloudiness than an average day.

6. THEORETICAL ANALYSIS

In this section, we will attempt to analyze the observed mean wind profile in terms of the customary equations

$$f(v-v_g)+\frac{1}{\rho}\frac{\partial \tau_{xz}}{\partial z}=0 \tag{1}$$

and

$$-f(u-u_g)+\frac{1}{\rho}\frac{\partial \tau_{yz}}{\partial z}=0. \tag{2}$$

Here, f is the Coriolis parameter, and ρ is an average value of the air density; τ_{xz} and τ_{yz} are the shear stresses associated with eddy transports of momentum along the vertical direction. The subscript g denotes the geostrophic value. It should be emphasized that the neglect of the accelerations while retaining the term fv in eq (1) and (2) may not be justified. At the latitude of Christmas Island, the Coriolis parameter is equal to 5×10^{-6} s^{-1}. Hence a horizontal shear in u along the north-south direction of 1 m s^{-1}/200 km would make the neglected term $v(\partial u/\partial y)$ equal to the Coriolis acceleration fv. This magnitude of the wind shear is so small that it is within the range of observational error. Lacking any firm empirical or theoretical estimates of the magnitudes of the local time and advective accelerations, we hypothesize that this is negligible in our analysis. Deductions from this analysis may indicate to what extent hypothesis is realistic.

The object of the analysis is to estimate the geostrophic wind components, u_g and v_g, and the stresses, τ_{xz} and τ_{yz}, from the observed wind profile by using eq (1) and (2). To obtain the estimates, we replace the vertical derivatives by finite differences with the aid of a vertical grid whose coordinates are $z_1, z_2, z_3, \ldots, z_n$. The first point, z_1, denotes the earth surface, $z=0$; the highest grid point is denoted by z_n.

We will assume that the geostrophic wind varies linearly with height such that

$$u_g=u_n+\alpha(z_n-z) \tag{3}$$

and

$$v_g=v_n+\beta(z_n-z) \tag{4}$$

which implies that, at $z=z_n$, the actual wind is equal to its geostrophic value.

In addition, we assume that the stress components at the surface are given by

$$(\tau_{xz})_1=\rho U_*^2 u_2(u_2^2+v_2^2)^{-1/2} \tag{5}$$

and

$$(\tau_{yz})_1=\rho U_*^2 v_2(U_2^2+v_2^2)^{-1/2} \tag{6}$$

where U_*, the friction velocity, is given by

$$U_*\equiv k_0(u_2^2+v_2^2)^{1/2}\left(\ln\frac{z_2+z_0}{z_0}\right)^{-1}$$

where z_0 is the roughness length and the subscript 2 indicates the value at the height z_2. These equations are derived with the aid of the mixing length theory and the logarithmic wind profile.

On the basis of these considerations, the finite-difference equations for eq (1) and (2) for the interval z_1 to z_2 are

$$f\left[\frac{v_1+v_2-2v_n-\beta(2z_n-z_1-z_2)}{2}\right]+\frac{(\tau_{xz})_2-(\tau_{xz})_1}{\rho(z_2-z_1)}=0 \tag{7}$$

and

$$-f\left[\frac{(u_1+u_2-2u_n-\alpha 2z_n-z_1-z_2)}{2}\right]+\frac{(\tau_{yz})_2-(\tau_{yz})_1}{\rho(z_2-z_1)}=0. \tag{8}$$

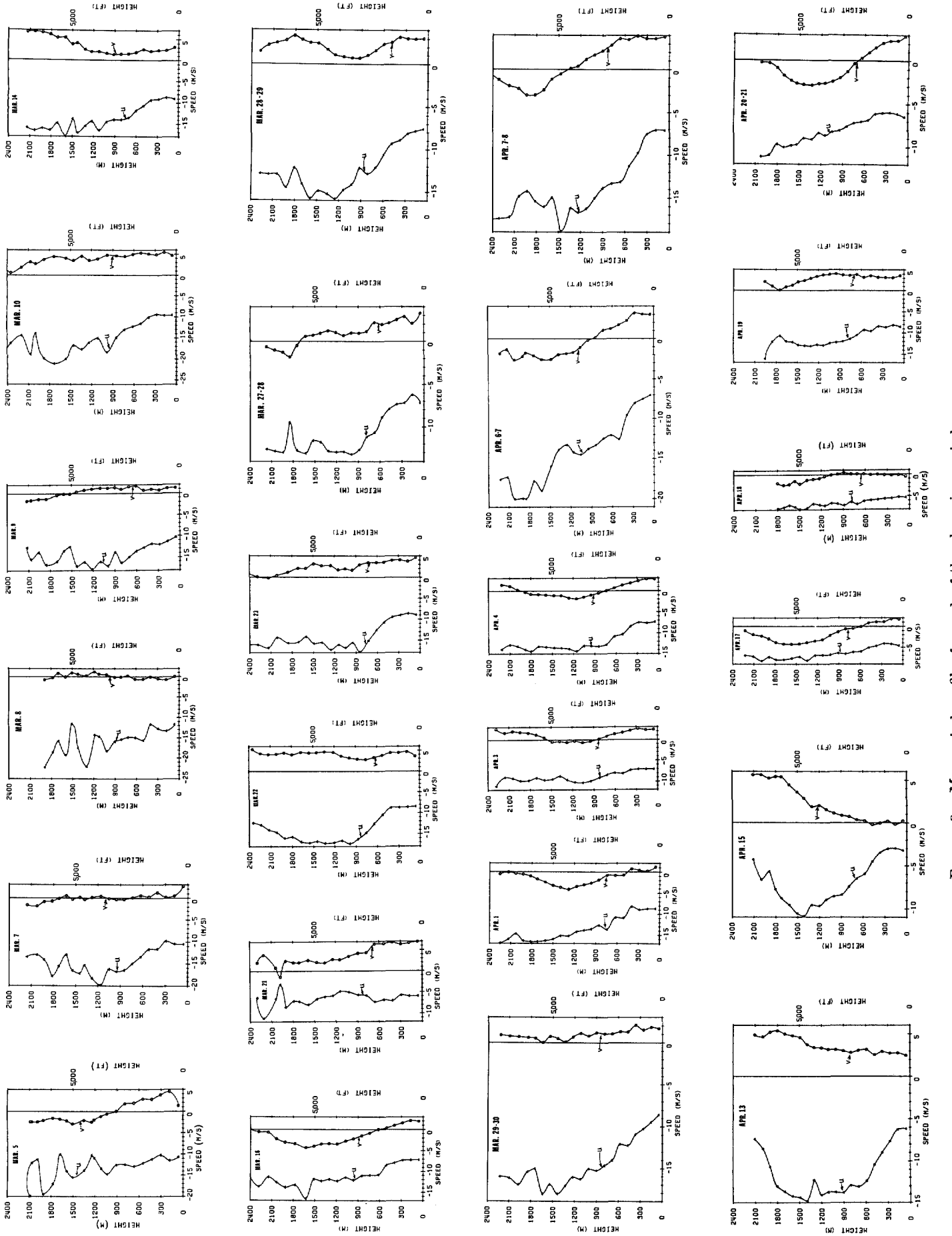

FIGURE 9.—Mean wind profiles for each of the observing periods.

TABLE 3.—*Heights of the grid points*

Grid point	z_1	z_2	z_3	z_4	z_5	z_6	z_7	z_8	z_9	z_{10}	z_{11}	z_{12}	z_{13}	z_{14}
Height (km)	0	0.1	0.2	0.3	0.4	0.5	0.6	0.7	0.8	0.9	1.0	1.1	1.2	1.3

Similar equations may be written for all remaining intervals, z_2 to z_3, z_3 to z_4, . . ., z_{n-1} to z_n. All these equations form a set of $2(n-1)$ simultaneous equations. The unknowns are the $2(n-2)$ stress components at z_2, z_3, . . ., z_n-1 plus α and β; the stress components at z_1 and z_n are regarded as known quantities.

The equations have been applied to the mean velocity components for all observations shown in figure 6. The heights of the grid points are shown in table 3.

In the applications, the wind stress components at the surface were estimated by specifying the roughness length in eq (5) and (6). According to a summary by Roll (1965), the roughness length of the sea surface is a function of the wind. Its values range from 10^{-7} to 10^{-2} cm. The value that is appropriate for our analysis is approximately 10^{-2} cm. At the highest grid point, z_{14}, both stress components were assumed to be zero. This is consistent with the fact that both u and v profiles show an extremum at about this height.

The results of the computations corresponding to the roughness length of 10^{-2} cm will now be discussed. The computed stress distribution is shown on figure 10. It may be seen that the magnitude of the shear stress decreases monotonically with height from a value of about 400 $cm^2 \cdot s^{-2}$ at the surface to zero at the top. The magnitude of the north-south stress component is on the average approximately 30 percent of the east-west component. This is consistent with the fact that the easterlies are stronger than the southerlies. Figure 11 shows the calculated hodograph of the geostrophic wind; also shown on the same figure is the mean wind used in the calculation. It may be seen that the geostrophic wind near the surface is almost twice that of the corresponding wind in magnitude. The latter blows toward lower pressure, making an angle of about 55° relative to geostrophic wind. The vector difference between the two, the ageostrophic wind, is of the same order of magnitude as either one near the surface. The magnitude of the ageostrophic wind decreases with height to zero at the top. It is clear from the diagram that the backing of the wind is simply a response to the variation of the horizontal pressure gradient with height.

The surface geostrophic wind implies a horizontal pressure pattern in which the isobars are oriented along a direction slightly west of due north with lower pressure to the west. The change in pressure per 500 km along a line normal to the isobars is about 0.4 mb. Using the thermal wind equation, one can estimate also the horizontal temperature gradient from the calculated geostrophic wind profile. On the basis of the geostrophic wind shear along the vertical, the isotherms would be oriented along the southwest to northeast direction, with higher temperatures to the northwest. The magnitude of the geostrophic wind shear gives a horizontal temperature gradient of about

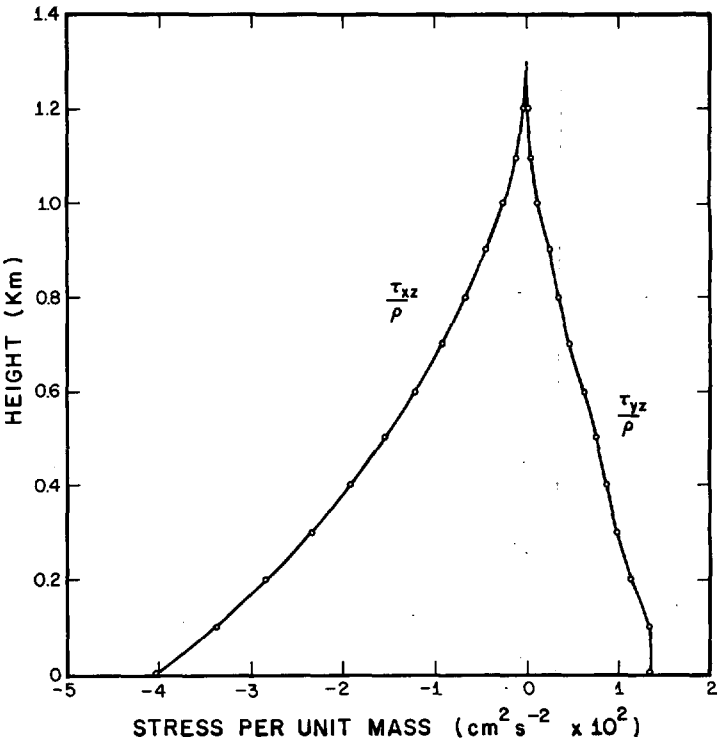

FIGURE 10.—Theoretical stress distribution ($z_0 = 10^{-2}$ cm).

0.8°C per 500 km. These computed values of horizontal surface pressure and temperature gradients imply that Fanning Island should be 0.1 mb lower in pressure and 0.9°F warmer than Christmas Island. The surface pressure and temperature observations at both islands gave differences of 1.0 mb and 2.2°F in which signs are the same as the computed values. It will be noted that the calculated pressure difference is only one-tenth that of the observed difference. The large discrepancy may be attributed to the neglect of acceleration terms in theoretical calculation. Or, it may be due to a systematic error in the surface pressure observations. Unfortunately, it is not possible to determine the source of the discrepancy on the basis of available information. The agreement between the calculated and the observed temperature differences is much better. The discrepancy of 1.3°F is certainly within the range of observational error.

Using the computed shear stress and the geostrophic wind distribution, we evaluated the magnitude of the terms of eq (1) and (2). Figure 12 shows the results. It may be seen that, along the east-west direction, the Coriolis force is so small that the balance of forces is mainly between the pressure gradient force and friction. This balance is similar to that found by Riehl et al. (1951) for the Northeast Trades. On the other hand, along the north-south direction, it is mainly between the Coriolis and the pressure gradient forces. Thus, the easterly component is approximately geostrophic. The force components in figure 12 have been combined vectorially to produce figure 13. This diagram shows that the magnitude of the pressure gradient force is almost constant with height. In contrast, the frictional force decreases with height while the Coriolis force increases with height.

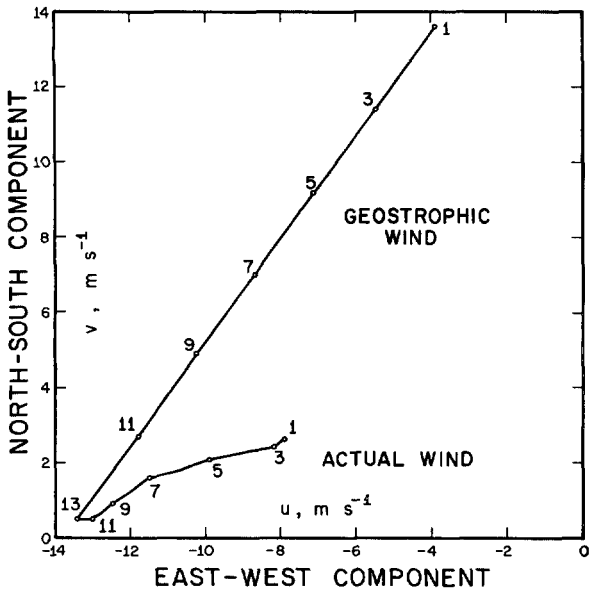

FIGURE 11.—Hodographs of the theoretical geostrophic wind ($z_0=10^{-2}$ cm) and the observed wind. The numbers indicate elevations in hundreds of meters.

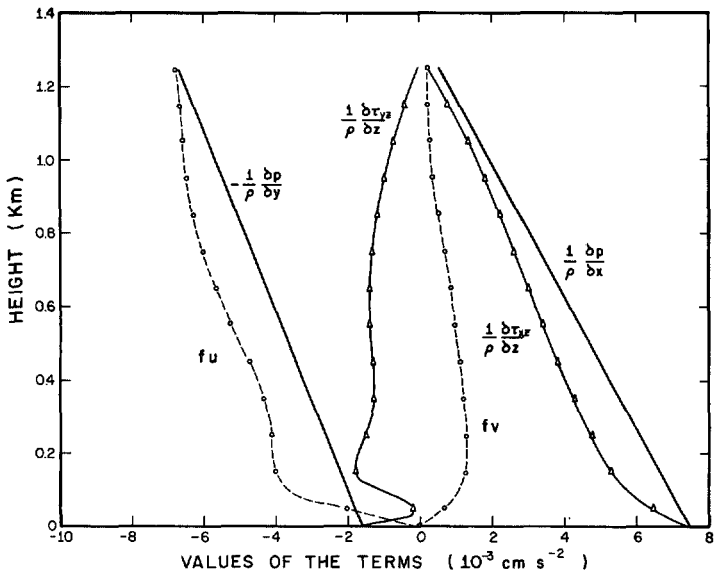

FIGURE 12.—Theoretical values of the terms of eq (1) and (2) for $z_0=10^{-2}$ cm.

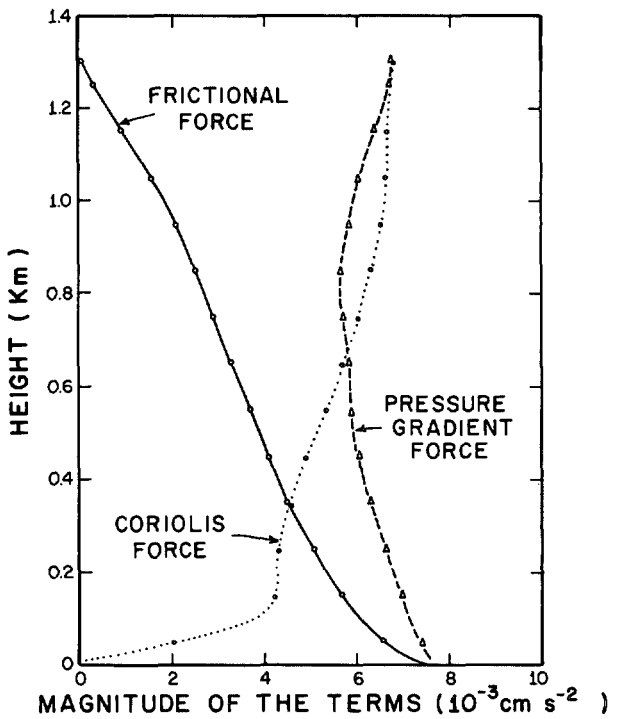

FIGURE 13.—Theoretical magnitudes of the Coriolis, friction, and horizontal pressure gradient forces for $z_0=10^{-2}$ cm.

TABLE 4.—*Dependence of various computed quantities on the roughness length*

Roughness length	cm	10^{-2}	10^{-3}	10^{-4}
Surface geostrophic wind speed	m s^{-1}	15	13	11
Surface geostrophic wind direction	deg.	167	158	150
Magnitude of thermal wind	m s^{-1} km^{-1}	12	10	8
Direction of thermal wind	deg.	36	40	44

Within the first few tens of meters from the surface, the pressure gradient force approximately balances friction, the Coriolis being negligible. Above the 1-km level, the balance is between the Coriolis and the pressure gradient forces. Near the 300-m levels, all three forces are equally important.

It is expected that the results of the analysis would depend on the magnitude of the roughness parameter that is used. To assess the sensitivity of the results to the specified values of the roughness parameter, we repeated the calculations for two other values, 10^{-3} and 10^{-4} cm. The results of these calculations, summarized in table 4, indicate that they are relatively insensitive to the roughness length.

7. CONCLUDING REMARKS

The primary objective of this study is to determine some of the important features of planetary boundary layer wind distribution over a homogeneous surface near the Equator. The pilot balloon observations at Christmas Island during the Line Islands Experiment has provided a good example of such a distribution. The wind is predominently easterly—with a small backing with height. The analysis of the wind observations indicate the following conclusions:

1. Near the Equator, the change in wind direction (backing or veering) with height is controlled mainly by the height variation of the horizontal pressure gradient.

2. The ageostrophic wind component is of the same order of magnitude as the actual wind within a deep layer that extends from the surface up to the 1-km level.

3. The equation of motion in the east-west direction reduces to a balance between the horizontal pressure gradient force and friction.

4. The equation of motion in the north-south direction reduces to the geostrophic wind balance, except for a thin layer near the surface. Thus, the easterlies are approximately geostrophic.

ACKNOWLEDGEMENTS

The author wishes to thank M. Sgt. Frank Harrison and the U.S. Army personnel for making the observations and Anton Chaplin for doing most of the data processing. The author is also grateful for the support of Dr. Edward Zipser and other scientists of the Line Islands Experiment who also provided some of the figures used in this article. This research was supported by the National Science Foundation under Grant GA–1021.

REFERENCES

Charnock, H., Francis, J. R. D., and Sheppard, P. A., "An Investigation of Wind Structure in the Trades: Anegada 1953," *Philosophical Transactions of the Royal Society of London*, Ser. A, Vol. 249, No. 963, England, Oct. 18, **1956**, pp. 179–234.

Riehl, Herbert, Yeh, Tu-cheng, Malkus, Joanne S., and LaSeur, Noel E., "The North-East Trade of the Pacific Ocean," *Quarterly Journal of the Royal Meteorological Society*, Vol. 77, No. 334, London, England, Oct. **1951**, pp. 598–626.

Roll, Hans U., *Physics of the Marine Atmosphere*, Academic Press, New York, N.Y., **1965**, 426 pp.

[Received April 30, 1970; revised August 20, 1970]